

# **Assessment of molten eutectic LiF-NaF-KF density through experimental determination and semi-empirical modeling**

**Ryan C. Gallagher <sup>a</sup>, Can Agca <sup>b</sup>, Nick Russell <sup>a</sup>, Jacob W. McMurray <sup>b</sup>, Nora D. Bull**

**Ezell <sup>a</sup> \*,**

<sup>a</sup> Nuclear Energy and Fuel Cycle Division, Oak Ridge National Laboratory, Oak Ridge, TN

37830

<sup>b</sup> Material Science and Technology Division, Oak Ridge National Laboratory, Oak Ridge, TN

37830

\*Corresponding author: bullnd@ornl.gov

## **Abstract**

Molten salts have favorable material properties for use in high-temperature energy systems, including thermal energy storage systems, concentrating solar power plants, nuclear reactors, and various industrial manufacturing processes. Knowledge of chemical and thermophysical property data is essential for the design and optimization of these systems, yet data is often limited or uncertain for many candidate salts due to the difficulty of thermophysical property measurements at relevant temperatures (e.g. 500-900°C). Here, the density of molten LiF-NaF-KF eutectic is re-assessed through review of previous experimental data, new density measurements from 470–800°C, and semi-empirical modeling. The density was measured using the displacement technique. Compositional and temperature-dependent density estimates

were calculated with a multidimensional Redlich–Kister model. The results of the new experimental measurements agree within 2% of the modeled density of molten eutectic LiF–NaF–KF. The Redlich–Kister model’s prediction shows a near ideal density behavior for the LiF–NaF–KF system and is promising for the estimation of off-eutectic LiF–NaK–KF densities. Lastly, through review of the existing literature and comparison to the new measurements, recommendations are made for the density of LiF–NaF–KF.

Key Points:

- Previous experimental measurements on molten eutectic LiF–NaF–KF were reviewed
- New measurements were taken using a displacement technique
- A Redlich–Kister model was used to provide predictions of LiF–NaF–KF density
- Empirical correlation for temperature-dependent density and the thermal expansivity of eutectic LiF–NaF–KF system is provided

## 1. Introduction

With growing energy consumption and the environmental impact of fossil fuel-based energy systems, the technological development and deployment of advanced clean sources of energy is essential to meet global energy demands while minimizing damage to the natural environment.

Molten salts exhibit promising properties for use in a wide array of advanced energy systems, all of which will require high operating temperatures. Applications include molten salt nuclear reactors,<sup>1</sup> high-temperature concentrating solar power plants,<sup>2–3</sup> sensible and latent thermal energy storage,<sup>4</sup> industrial waste heat recovery,<sup>5</sup> and carbon capture.<sup>6</sup> Fluoride- and chloride-based molten salt mixtures have high volumetric heat capacities, reasonable thermal conductivity, low vapor pressures, high temperature stability, and high boiling points. The combination of all these

qualities make them ideal candidates for systems with working temperatures of 400°C and higher, a characteristic that is in contrast with nitrate-based molten salts that are currently being deployed in existing solar energy systems and have lower maximum operating temperatures (~560°C).<sup>7-8</sup> Fluid systems with higher operating temperatures can enable improved efficiency through coupling with supercritical CO<sub>2</sub> Brayton power cycles.<sup>7, 9</sup> Despite the existing applications of molten salts in thermal energy systems and their proposed use in higher-temperature advanced energy systems, issues still exist for these materials that limit technological development and eventual deployment.

One factor limiting the development of these high-temperature fluid systems is insufficient knowledge of temperature-dependent thermophysical and chemical properties for many salt mixtures.<sup>10</sup> Although a variety of molten salts may be used in different energy systems, all systems will require knowledge of the salt mixture's thermophysical properties for the design and optimization of components. For example, density is required for estimating thermal storage capacity, as well as mass flow calculations.<sup>11</sup> Despite this need and because of the difficulty of performing accurate measurements, reference-quality experimental property data for many multicomponent molten salt systems are either lacking or conflicting.<sup>12-16</sup> Complicating factors such as hygroscopicity, corrosivity, volatility, and the tendency to wet out from experimental containers can severely bias the results of experimental techniques.<sup>17-19</sup> Furthermore, a significant amount of existing data also lack rigorous detail on salt preparation/purification, compositional verification, testing environment, and post-measurement analysis due to the dearth of standard practices for handling and measurement that have been applied and validated on a variety of molten salt mixtures.

Semi-empirical models capable of estimating the properties of high-order molten salt mixtures can be used to bridge the gap between existing experimental data and to provide predictions of multicomponent systems. The Redlich–Kister (RK) expansion has been previously applied for empirical property predictions of density by extrapolation on endmember and pseudo-binary salt mixtures.<sup>20</sup> These semi-empirical models provide a tractable formulation that can be easily integrated into thermal systems codes and analysis software, allowing the community to readily evaluate properties of different salt mixtures.<sup>10,21</sup> RK and similar semi-empirical models also have the potential to be used in data screening efforts that focus on the identification of errant, outlier data in pseudo-binary or higher order mixtures.

The work presented here uses experimental measurements, RK model estimation, and a review of existing data to assess the density of ternary molten salt consisting of eutectic LiF-NaF-KF (46.5-11.5-42 mol%), commonly referred to as FLiNaK. The LiF-NaF-KF system was selected as a potential reference material for validation and verification of existing and novel experimental techniques because of its relevance to advanced energy systems and relatively mature body of work compared to other systems.<sup>22-23</sup> Lastly, this work provides recommended property data that can be implemented in chemical and thermophysical databases that are essential for the modeling and simulation of energy systems that utilize molten salts as heat transfer fluids.<sup>21</sup>

## **Review of Existing Data**

Molten salts have been studied for decades, and many reviews, databases, and reports already exist. However, many databases may not contain reference quality data. Fluoride molten salts were extensively studied at the Oak Ridge National Laboratory (ORNL) as a possible coolant fluid for molten salt reactors under the Molten Salt Reactor Experiment Program (MSRE); thus, experimental data, purification techniques, and handling procedures have already been detailed in

numerous technical reports. Unlike many other salt systems, LiF-NaF-KF experimental data are generally more widely available and have been critically reviewed by multiple sources.<sup>14-16, 22-23</sup> Therefore, LiF-NaF-KF is proposed as a reasonable starting point for qualifying measurement and modeling methods. However, there are still several considerations when evaluating the quality of existing data and when collecting new experimental data. For example, many molten salt mixtures are highly hygroscopic, and handling must be performed in dry, oxygen-free environments as impurities can lead to corrosive behavior which in turn influences the thermal properties of the salt.<sup>24-25</sup> Unfortunately, purity and preparation details are also missing in literature. Therefore, existing data were reassessed to provide adequate comparison to measurements provided herein.

## **Density**

Density is a key property for assessing the thermal transport capacity of fluids in both forced and natural convection systems. Generally, measuring the density of molten salts is straightforward, and numerous sources have reported or recommended LiF-NaF-KF density values. However, there is a relative dearth of experimental measurements of density that provide detail on the experimental procedure and setup. Even fewer studies have provided detailed discussion on the sample preparation, chemical characterization technique, and details on the uncertainty quantification. This missing discussion calls the quality of the data resulting from those studies into question.

The earliest referenced measurement of LiF-NaF-KF density was provided in 1954 by Cohen and Jones,<sup>26</sup> Many references can be linked back to that original data including Grimes et al.,<sup>27</sup> Powers in 1963,<sup>28</sup> Vreisema in 1979,<sup>29</sup> Williams in 2006,<sup>14</sup> Ambrosek et al. in 2009,<sup>30</sup> Holcomb and Cetiner in 2010,<sup>31</sup> and Yoder in 2014.<sup>32</sup> However, the reported uncertainty of 5% (assumed to be 0.05 relative standard uncertainty) by Cohen and Jones<sup>26</sup> is relatively high compared to more recent measurements and therefore the results listed by Cohen and Jones should be reconsidered as a

reference source. Later, a density measurement was reported by Mellors and Senderoff in 1965.<sup>33</sup> The Mellors and Senderoff data were referenced by Janz and Tompkins.<sup>34</sup> Like Cohen and Jones, the experimental data from Mellors and Senderoff have been referenced in other works<sup>35-36</sup> and critically recommended as reference data by Benes and Konings<sup>22</sup> as well as Serrano-Lopez et al.<sup>15</sup> These recommendations were due to its near-ideal density and strong agreement with experimental data from Chrenkova et. al.<sup>35</sup> and Cibulková et al.,<sup>36</sup> which both presented the same linear empirical correlation of density with temperature. However, a few more recent works have reported data on the density of LiF-KF-NaF,<sup>37,38-40</sup> all of which show similar expansion terms but higher density values than the Janz correlation—however, they fall within a 2% margin, which corresponds to the uncertainty suggested by Janz. Note that Barborik et al.<sup>40</sup> reported a relatively large expansion term compared to the other works (aside from Cohen and Jones<sup>41</sup>), but agrees well with the works that postdate Cibulková<sup>36</sup>. Other works have also used computational modeling through molecular dynamics simulation and first principles to predict the density of molten LiF-NaF-KF,<sup>42-43</sup> but these were not considered here as the scope is limited to experimental measurements. Table 1 lists the details of the previous density measurements. Note that more recent experimental measurements have reported relative standard uncertainties of <0.01 on their density values, an expected improvement in comparison to earlier measurements. Additionally, only Cheng et al.<sup>38</sup> and Rose et al.<sup>39</sup> include detail on purification, characterization and surface tension correction.

**Table 1:** Previous experimental measurements of molten eutectic LiF-NaF-KF density with details on the measurement method and materials, the reported experimental temperature range, and the measured temperature dependent density in the form  $\rho = a - b \cdot T$ , and the standard

uncertainty. Here, a and b are the reported fitting constants.  $\rho$  is the density in g/cm<sup>3</sup>, and T is the temperature in °C.

Reference	Method/Materials	Temperature Range	Reported Density Constants	Standard Uncertainty <sup>a</sup>
Cohen, 1954 <sup>26</sup>	Materials: Stainless steel plummet, crucible, and wire Purification: not mentioned Surface tension: not mentioned Characterization: not mentioned	600–900	a = 2.5297 b = 7.30e-4	0.05
Mellors, 1965 <sup>33-34</sup>	Materials: tungsten plummet Purification: not mentioned Surface tension: discussed Characterization: not mentioned	675–900	a = 2.4089 b = 6.240e-4	0.02
Chrenkova, 2003 <sup>35-36</sup>	Materials: Pt wire, plummet, and crucible Purification: not mentioned Surface tension: not mentioned Characterization: XRD, IR spectroscopy	660–890	a = 2.4089 b = 6.240e-4	0.004
Cheng, 2013 <sup>38</sup>	Materials: Pt plummet and wire, BN or graphite crucible Purification: not mentioned Surface tension: corrected Characterization: pretesting OCP-OES	500–625	a = 2.4344 b = 6.41e-4	0.003
Barborik, 2014 <sup>40</sup>	Materials: Pt crucible (wire and plummet not mentioned) Purification: vacuum drying Surface tension: correction not mentioned, but it was measured Characterization: XRD	485–625	a = 2.4649 b = 6.92e-4	0.001
An, 2017 <sup>37</sup>	Materials: Pt plummet <sup>38</sup> Purification: argon drying, melted for homogenization Surface tension: corrected Characterization: pretesting XRD	480–700	a = 2.45 b = 6.53e-4	-
Rose, 2020 <sup>39</sup>	Materials: Ni crucible and plummet Purification: not mentioned, production reports cited Surface tension: corrected Characterization: pretesting XRD and ICP-OES	500–750	a = 2.44 b = 6.06e-4	0.005

<sup>a</sup> relative standard uncertainty is assumed when not specified by author

## 2. Experiment Methods and Materials

### Sample Preparation Methods

As impurities in molten salt have been linked to increased corrosion rates<sup>24-25</sup> and may potentially lead to biased measurements in some molten salt mixtures, the purity of the samples must be characterized before analysis.<sup>44</sup> LiF-NaF-KF and other fluoride salts can be purified through fluorination with anhydrous hydrofluoric acid (hydrofluorination) to remove water, oxide, and

hydroxide impurities from the salt.<sup>45-47</sup> The LiF-NaF-KF analyzed in this work was purified by hydrofluorination completed by Electrochemical Systems, Inc. using procedures developed at ORNL.<sup>45</sup> Specific details regarding the purification process are not publicly available. However, as noted by Sulejmanovic et al., previous corrosion tests and ICP-OES analysis on a sample from this batch indicated low levels of impurities.<sup>48</sup>

The purity of the salt sample used in these measurements was characterized through combustion analysis on two LECO ONH836 instruments, oxygen hot extraction, inductively coupled plasma mass spectrometry on a Thermo Scientific Finnigan Element 2 instrument, glow discharge mass spectrometry, and capsule corrosion experiments. Additional detail on the salt characterization is described in Sulejmanovic et al.<sup>48</sup> Table 2 summarizes the details on the sample chemistry, purification, and purity adapted from Sulejmanovic et al. The salt samples used in the measurements discussed herein were prepared and stored in argon (Ar) gloveboxes at 0.4 ppm oxygen concentration and 0.1 ppm moisture levels or lower. Preparation included loading the salt into the crucibles and sealing it inside Ar vials for transport to the instruments, when necessary. In the case of the density measurement system described herein, the full apparatus is located inside an Ar glovebox.

**Table 2:** Summary of sample chemistry, purification, and purity adapted from<sup>48</sup>

<b>Sample</b>	<b>Mol%</b>	<b>Purification</b>	<b>O (µg/g)</b>	<b>H (µg/g)</b>	<b>Impurities (µg/g)</b>
LiF-NaF-KF	46.5-11.5-42	Hydro-fluorination <sup>a</sup>	1459 ± 421 <sup>b</sup> 212.5 ± 81.0 <sup>c</sup>	22.9 ± 7.8 <sup>b</sup>	806.3 <sup>d</sup>

<sup>a</sup> purified LiF-NaF-KF supplied by Electrochemical Systems Inc.

<sup>b</sup> measured by combustion analysis, standard uncertainty

<sup>c</sup> measured by oxygen hot extraction, standard uncertainty

<sup>d</sup> measured by inductively coupled plasma mass spectrometry, uncertainty not reported

## Density Measurement Method

The displacement technique, or Archimedes method, has been widely applied to determine the densities of liquids and solids, and it is often used to measure molten salts.<sup>16</sup> The weight of a solid plummet, measured in a known gas, is compared to the weight while submerged in the fluid sample being measured. The force applied on the plummet while submerged is equal to the weight of the displaced liquid. Therefore, the density of the fluid can be determined by dividing the weight difference over the volume of the plummet. At high temperatures, Eq. (1) is used to correct for the effects of the plummet's thermal expansion, as well the surface tension force exerted on the suspension wire by the fluid.<sup>37-39, 49</sup> The density of the fluid ( $\rho_{fluid}$ ) is

$$\rho_{fluid} = \frac{w_0 - w_{fluid} + \frac{\pi D \sigma \cos(\theta)}{g}}{V[1 + \alpha(T - T_{ref})]^3}, \quad (1)$$

where  $w_0$  is the weight of the plummet outside of the fluid,  $w_{fluid}$  is the weight of the plummet measured while submerged in the fluid,  $D$  is the diameter of the suspension wire,  $\sigma$  is the surface tension of the fluid,  $\theta$  is the contact angle,  $V$  is the volume of the plummet,  $T$  is the temperature of the fluid,  $\alpha$  is the coefficient of thermal expansion (CTE) of platinum,<sup>50</sup>  $T_{ref}$  is the reference temperature of the CTE, and  $g$  is gravitational acceleration.

The surface tension correction depends on the wetting properties of the wire and can exert forces with or against the direction of gravity depending on the wire-fluid contact angle.<sup>49</sup> Molten salts generally exhibit highly wetting behavior on metallic surfaces and would thus have contact angles of  $<90^\circ$ , exerting a force in the direction of gravity. However, contact angles are dependent on the material and surface roughness of the wire, so additional consideration may be necessary when

correcting for the surface tension effect. In practice, the surface tension effect has been assumed to be nearly zero for molten salt measurements, which corresponds with complete wetting.

A custom apparatus, installed in an Ar glovebox at ORNL, was used for density measurements. The current system employs a platinum plummet suspended from the bottom of a precision balance by a thin metal wire. The balance is located on a stand above the glove box's thermal well, which contains a three-zone tube furnace. The thermal well is cooled by recirculating chilled water lines positioned on the outside surface. This maintains the glovebox temperature at an adequate operating temperature while the furnace is running. The specimen is contained within a cylindrical 316 stainless steel crucible that holds the specimen at the furnace axial midplane, where the temperature is the most temporally stable and axially uniform. **Figure 1:** Depiction of the Archimedes density system with the furnace located outside of the glove box's thermal well. Figure 1 shows the density apparatus when operated outside of the glovebox's thermal well.

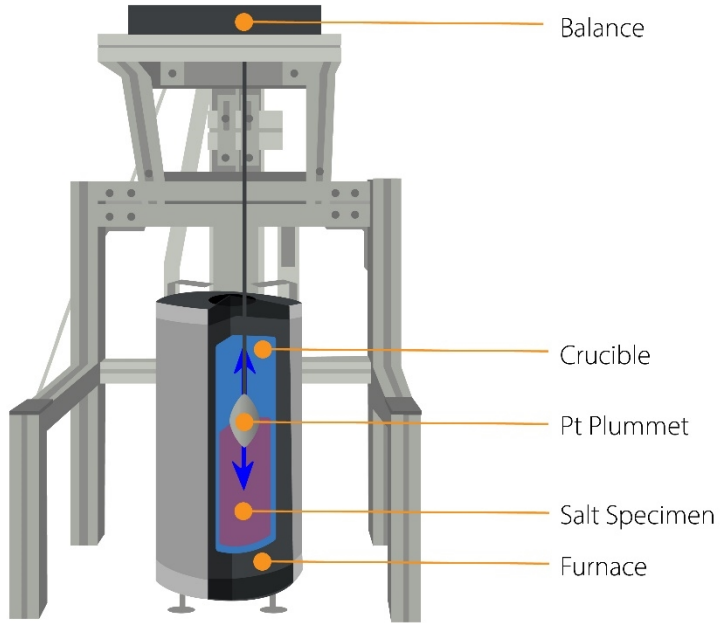


**Figure 1:** Depiction of the Archimedes density system with the furnace located outside of the glove box's thermal well.

### Property Estimation Methods

To estimate the density of LiF-NaF-KF, a model using RK expansion was applied.<sup>51</sup> The methodology for density estimation is explained by Agca et al.<sup>20</sup> and McMurray et al.<sup>10</sup> Accordingly, the density equation for the liquid mixture ( $\rho_{\text{mix}}$ ) is composed of two terms: the ideal and excess behavior. Equation (2) shows the density of the molten salt mixture.

$$\rho_{\text{mix}} = \rho_{\text{id}} + \rho_{\text{ex}} \quad . \quad (2)$$

The ideal behavior term ( $\rho_{\text{id}}$ ) comes from the additive nature of the volume as a physical property, whereas  $\rho_{\text{ex}}$  is the term to account for the deviation from the ideal density behavior. Similar equations to Eq. (2) were used in the past, where an ideal term was determined directly from volume.<sup>35, 52-53</sup> Ideal density is calculated as the ratio of average molecular weight to the molar volume of the liquid:

$$\rho_{id} = \frac{\sum x_i MW_i}{\sum \frac{x_i MW_i}{\rho_i}}, \quad (3)$$

where  $MW_i$  is the molecular weight and  $x_i$  is the molar fraction of component  $i$ . The excess behavior of the density of molten salts is defined using the RK expansion.<sup>51</sup> It has been widely used to describe the Gibbs free energy functions in the CALPHAD method.<sup>54</sup> The excess density behavior term via the RK model is

$$\rho_{ex} = x_a x_b \sum_{j=1}^n L_j (x_a - x_b)^{j-1}. \quad (4)$$

Here,  $j$  defines the order of the expansion, and  $L_j$  is the  $j$ th order density interaction parameter between pure salt compounds  $a$  and  $b$ . Although an equation with various temperature-dependent terms can be used,  $L_j$  is described by a linear temperature-dependent function (Eq. 5) given the expectation that density varies linearly with temperature:

$$L_j = A_j + B_j T \quad (5)$$

Temperature units are in Kelvin for Eqs. (2–5). Ternary systems have been modeled using the approach outlined here. The ternary interaction parameter of the KF-LiF-NaF system is considered negligible, which agrees with typical RK modeling practices at a single temperature applied to other ternary molten systems.<sup>36, 55–56</sup> Equation (6) shows a typical RK expansion for a ternary system.

$$\rho_{ex} = x_a x_b \sum_{j=1}^n L_j (x_a - x_b)^{j-1} + x_a x_c \sum_{j=1}^n L_j (x_a - x_c)^{j-1} + x_b x_c \sum_{j=1}^n L_j (x_b - x_c)^{j-1} \quad (6)$$

The binary interaction parameters are estimated using a multidimensional nonlinear least squares method. MATLAB's curve fitting tool with Trust Region and Levenberg–Marquardt<sup>57–58</sup> algorithms have been used in the calculations. Higher convergence of the fit to the reference data

was achieved using a least absolute residual robust method in the case of KF-NaF. Reference data were taken from Taniuchi et al.<sup>59</sup> for a KF-LiF system, Porter and Meaker<sup>60</sup> for a KF-NaF system, and Janz's reference database for a LiF-NaF system.<sup>61</sup> Pure densities were selected as in Table 3 and used in the modeling and ternary extrapolations for consistency. Further details of the modeling and calculations are explained in Agca et al.<sup>20</sup>

**Table 3 :** Densities used in the modeling and ternary extrapolations for the KF-LiF-NaF system

Pure Salt	Density Equation [g/cm <sup>3</sup> ], T in K	Source
KF	$2.6616 - 6.6500 \times 10^{-4} T$	<sup>59</sup>
LiF	$2.3289 - 4.6803 \times 10^{-4} T$	<sup>61</sup>
NaF	$2.6820 - 6.1510 \times 10^{-4} T$	<sup>60</sup>

### 3. Results and Discussion

#### Experimental Density Results

Density measurements were initially made at 470°C after being held for 15 minutes above the melting point to let the salt homogenize. The rest of the measurements were made in increasing increments 100 K from 500°C, up to 800°C. Measurements at each given temperature started once the measured mass fluctuations on the balance were less than 0.005 g. Four separate weight measurements were recorded at each temperature point separated by approximately 15 minutes. The average value of the four measurements and the calculated uncertainties were calculated via propagation of errors and are listed in Table 4. The calculated densities assumed a contact angle of zero degrees, which is reasonable given the expected wetting behavior of LiF-NaF-KF eutectic on metals. With the large plummet mass (105.621 g) and small wire diameter (0.254 mm), the uncertainty in a contact angle of 90° would result in measured densities around 1% lower than

what is listed in Table 1. The largest source of experimental uncertainty was balance instability. The four separate measurements demonstrated deviations as high as  $\pm 0.02$  g, despite the balance having a calibrated accuracy of  $\pm 0.1$  mg. The deviations in balance measurements were largest ( $\pm 0.02$  g) at 470°C, and it was noted that the measured weight decreased with time, suggesting that the deviation could have been caused by non-equilibrium conditions in the salt which may not have been fully homogeneous at the lower temperatures.

**Table 4:** The measured density of LiF-NaF-KF eutectic (gauge pressure = 200 Pa)

T [°C]	$\rho$ [g/cm <sup>3</sup> ]	Uncertainty <sup>a</sup>
470	2.177	0.0042
500	2.155	0.0045
600	2.065	0.0020
700	2.008	0.0023
800	1.954	0.0014

<sup>a</sup> Uncertainty reported as standard relative uncertainty

These measured results are closest to those of Rose<sup>39</sup> and Cohen and Jones,<sup>26</sup> especially within the range of 600–800°C. Our measured results were around 1% higher than those of other works that also feature surface tension corrections<sup>37-38</sup> as well as Barborik et al.<sup>40</sup> The results deviated by around 2% compared to the density reported by Cibulková et al.,<sup>36</sup> Chrenkova et al.,<sup>35</sup> and Mellors.<sup>33, 61</sup> The former three works do not mention corrections for surface tension. Furthermore, the Mellors data, which does consider surface tension, has a reported relative uncertainty of 0.02 (assumed to be standard uncertainty). This uncertainty range covers the other experimental data collected here. As noted by Rose et al.,<sup>39</sup> these small deviations between different measurements may be minor enough to be caused by effects of surface tension, salt compositional makeup, purity, and assumed plummet expansion coefficients. Nonetheless, due to the agreement with the more recent works of Cheng et al. and Rose et al.—which both feature surface tension corrections—

these works, along with the present study, are recommended as primary reference data for the density of molten eutectic LiF-NaF-KF.

The thermal expansion coefficient of the LiF-NaF-KF eutectic molten salt was calculated using a least squares fit on the measured data with respect to temperature. The fit line of density in grams per cubic centimeter is expressed as  $2.492 - 6.846\text{e-}4 \times T$ , in  $\text{g}/\text{cm}^3$  and  $T$  in  $^{\circ}\text{C}$ . This fit has a coefficient of determination of 0.988 and a maximum relative deviation from the measured values of 0.77%. Using this fit, the volumetric thermal expansion coefficient was calculated as  $3.5\text{e-}4 \text{ K}^{-1}$ .

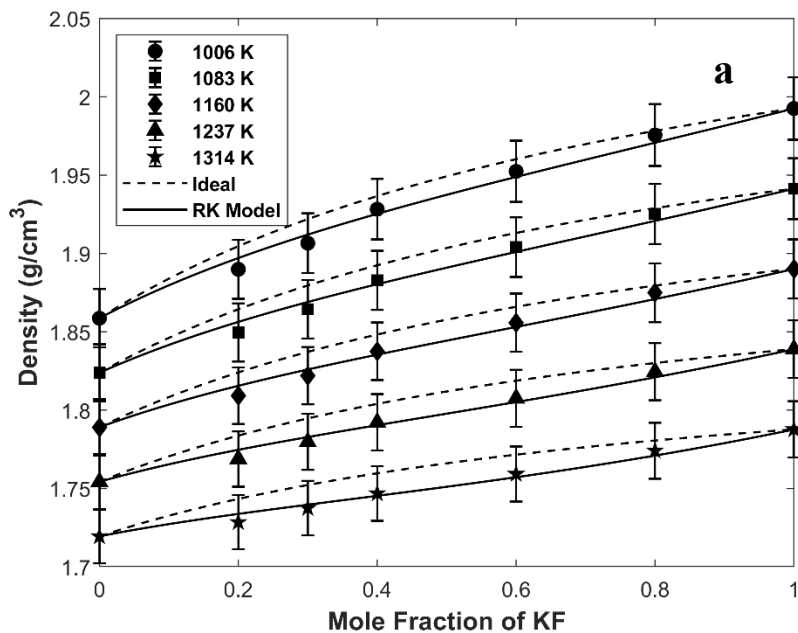
## Property Estimation Results

Binary density interaction parameters,  $L_j$ , calculated using the RK model, are shown in Table 5. Fitting parameter  $A_1$  in Eq. (5) is the dominant term in the determination of how far away the density is from the ideal behavior. For an  $A_1$  value smaller than 0.5, one can suggest a close-to-ideal behavior for engineering design purposes. KF-LiF and LiF-NaF systems have had a slight negative deviation from ideality ( $\leq 1\%$ ), almost indistinguishable from ideal behavior (Figure 2a, c). Given the small interaction parameters for KF-LiF and LiF-NaF, near ideal behavior could be suggested for these two pseudo-binaries. However, the KF-NaF system has peculiar density data on the KF-rich side. Between 75 and 90 mol % of KF, the expansion coefficient for the molten salt mixture drops unusually (Figure 2b). This behavior may not necessarily be associated with the eutectic effects since the eutectic is on 60 mol % KF.<sup>62</sup> It is possible that measurement errors on the reported KF-rich salt mixtures lead to this apparent drop in the expansion coefficient in KF rich mixtures. We therefore suggest that new density measurements be taken on KF-rich KF-NaF mixtures, but a compositional study is outside of the scope of this work. The least absolute residual robust algorithm reduces the effects of suspected KF-rich compositions, but still results in an 8%

relative deviation from reference data.<sup>60</sup> However, in the context of this study (eutectic LiF-NaF-KF), the density behavior should be considered as close to ideality given the lower binary interaction parameters of KF-LiF and LiF-NaF, relative to KF-NaF.

**Table 5:** Binary interaction parameters for density in KF-LiF, KF-NaF and LiF-NaF systems

Binary System (Salt A – Salt B)	$L_1$	
	$A_1$	$B_1$
<b>KF-LiF</b>	-0.005383	$-4.1427 \times 10^{-5}$
<b>KF-NaF</b>	-0.3748	$2.3540 \times 10^{-4}$
<b>LiF-NaF</b>	-0.06998	$1.0739 \times 10^{-5}$



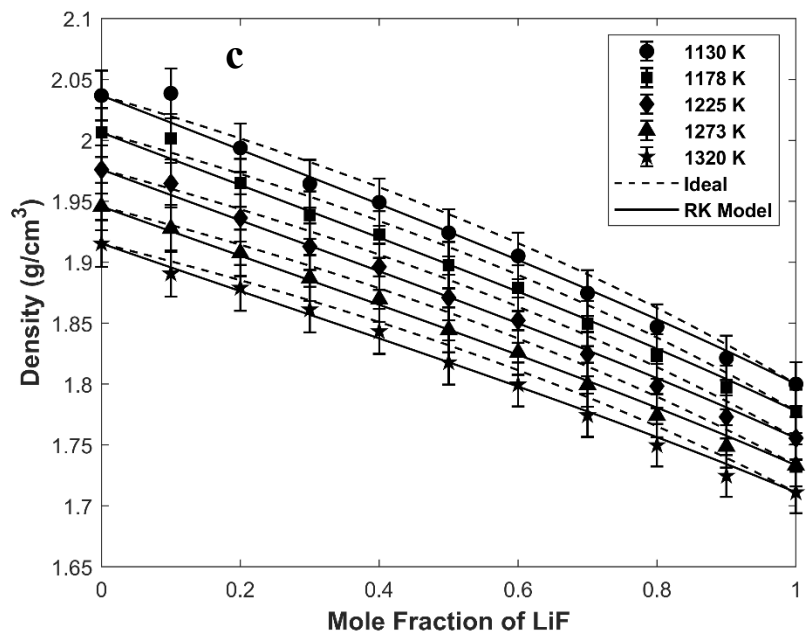
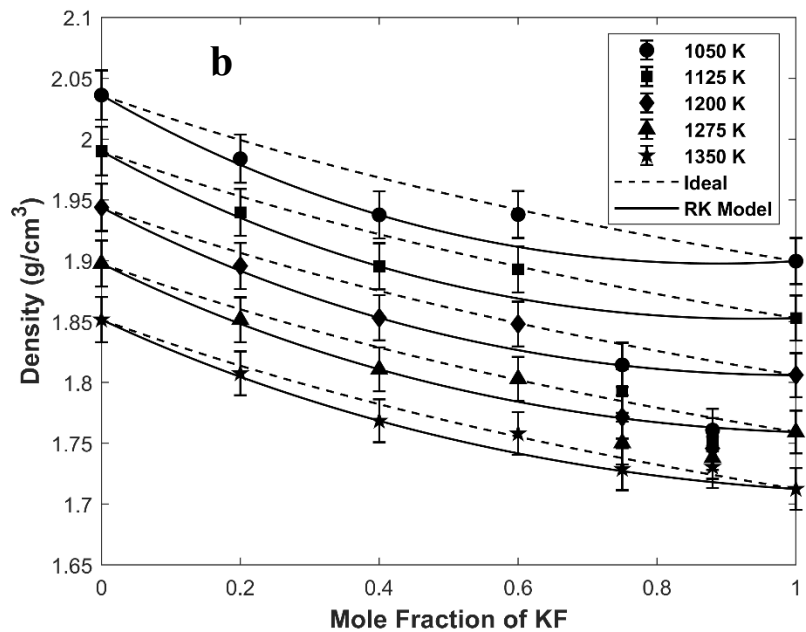


**Figure 2:** The comparison between the ideal behavior, RK model, and reference data in a) KF-LiF;<sup>59</sup> b) KF-NaF;<sup>60</sup> and c) LiF-NaF<sup>61</sup> pseudo-binary fluoride systems constituting the LiF-NaF-KF mixture (1% error bars on the reference data)

Density extrapolations of LiF-NaF-KF were performed using Eq. (6) using the binary interaction parameters in Table 5. The extrapolation temperature range was dependent on the minimum and maximum reference temperature in the binary systems. Accordingly, LiF-NaF-KF composition (46.5 mol % LiF, 11.5 mol % NaF, and 42 mol % KF) density was estimated from 1006 to 1350 K, for which the minimum temperature boundary is about 279 K above the melting temperature of LiF-NaF-KF.<sup>41</sup> Furthermore, density assuming ideal behavior has also been calculated assuming the binary interactions are zero. Figure 3 compares ideal behavior, RK model density results, and reported experimental values.

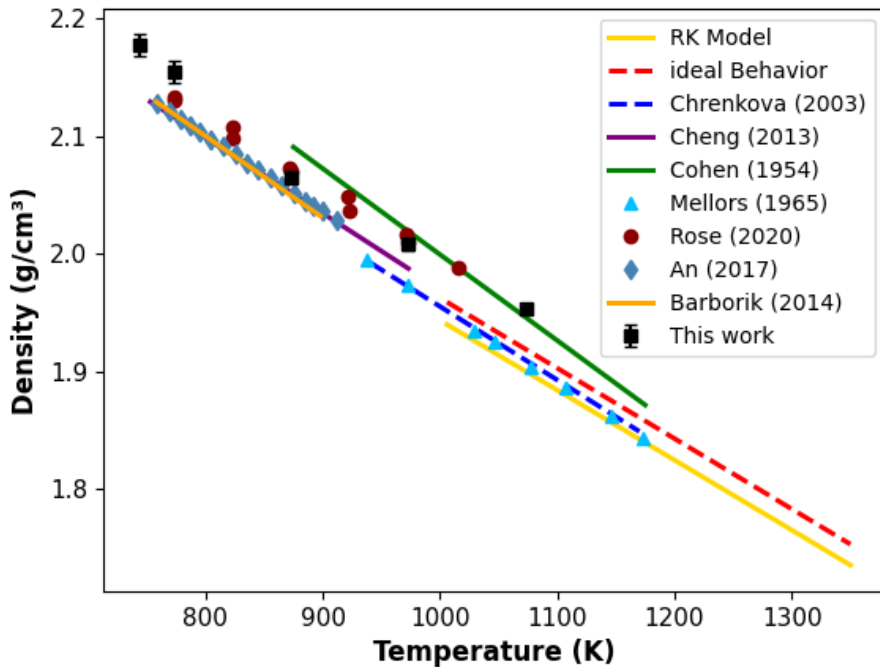


**Figure 3:** The measured and estimated density of LiF-NaF-KF eutectic in comparison with previously reported experimental data

The extrapolated ideal and RK model density estimations agree well, within 1% and 1–2% respectively, with earlier reported values above 1006 K.<sup>26, 33, 35-36</sup> The higher negative deviation on of the RK model result suggests that, using the selected pure and pseudo-binary density data, the

LiF-NaF-KF density might be better represented with the ideal extrapolation. Furthermore, ideal behavior density shows good agreement, within 1.5–2% relative deviation, with low-temperature density reports, including our measured results. This suggests that the ideal behavior density could be used across a wide temperature range to predict the LiF-NaF-KF density with reasonable accuracy. These results also demonstrate that the pure molten salt density data could be used for ideal extrapolation to ternary and higher order mixtures when there is considerable ideal behavior.

The RK model predicted a lower density than what was measured here, reported in previous experimental studies, and predicted with the ideal extrapolation. It is also of note that both models predict lower densities than those shown from the results from our experimental measurements. This may be a result of errors in the experimental input data used by the two models. As already discussed, the experimental results depend on correctly accounting for surface tension effects and thermal expansion of the plummet. Therefore, it is possible that the pure component and pseudo-binary data may not have made the same corrections as the present measurement. One example supporting this conclusion is the fact that the experimental data that considered surface tension (this work, Rose et al.<sup>39</sup>, and Cheng et al.<sup>38</sup>) was generally higher than the data that excluded surface tension corrections (Cibulková et al.<sup>36</sup> Chrenkova et al.<sup>35</sup>). Our experimental data also agrees well with Barborik et al.<sup>40</sup>, though limited details were given on the density measurement for that work. Additionally, the thermal expansion term reported by Barborik et al.<sup>40</sup> is higher than most other experimental works. If surface tension corrections were not applied to the pure or pseudo-binary data, the RK and ideal extrapolation models will both predict densities that are lower than what was measured. It should also be noted that a 2% margin of error is on the order of the experimental error margins reported by the early density measurements, as summarized in Table 1.

Another potential cause for the underprediction, with the RK model specifically, is the use of KF-NaF pseudo-binary data, which exhibited relatively significant negative deviations from ideality for KF-rich mixtures. This would result in an underprediction of the ternary density following extrapolation. Since the pseudo-binary data is a necessary input for the RK model, additional experimental investigations of KF-rich mixtures of KF-NaF may be necessary if improved accuracy is desired. Though, a compositional study is outside the scope of this work. It should also be noted that 2% error is on the order of experimental error for early density measurements, as summarized in Table 1, so the agreement between the predicted density of eutectic LiF-NaF-KF using the RK and ideal extrapolation models and experimental data is still reasonably accurate. Therefore, both models could be considered acceptable for estimating the compositional and temperature dependent density of the LiF-NaF-KF system, but the RK expansion is still expected to have higher accuracy when applied to other mixtures that feature non-ideal behavior.<sup>20</sup>

#### 4. Conclusions

The density of the eutectic of the LiF-NaF-KF system was studied experimentally with the displacement technique. The mixture's density was also estimated using Redlich–Kister expansion-based semi-empirical extrapolations from existing data on the pure components and pseudo-binary mixtures. The new experimental data showed good agreement (1% relative deviation) with comparatively recent density measurements from literature that included surface tension corrections. Given the agreement, this work, Rose et al.<sup>39</sup>, and Cheng et al.<sup>38</sup> are recommended as reference data for molten eutectic LiF-NaF-KF. The density predicted with the RK model agrees well, within 2% of our recommended experimental data. The RK and ideal extrapolation model predicted lower densities compared to our recommended experimental data,

with the ideal extrapolation having slightly lower deviations, which may be a result of errors in the RK model's input data.

Discrepancy between the recommended experimental and RK estimated data suggests that the pure or pseudo-binary data may need to be evaluated further—namely, the KF-rich mixtures of KF-NaF—because the RK technique is limited by the quality of the pure and pseudo-binary input data. The input references would require further review if improved accuracy with the RK technique is desired. Together, experimental and semi-empirical estimations using RK are promising for characterizing the density of multicomponent fluoride molten salts, offering a solution to collect and analyze data for the development of molten salt density data that can be utilized by industry as well as in the development of property databases.

### **Acknowledgements**

The authors acknowledge the assistance at ORNL of Dino Sulejmanovic for chemical impurity analysis of the salt sample, reviewers of the manuscript. This research was funded by The U.S. Department of Energy, Office of Nuclear Energy, Molten Salt Reactor Campaign.

### **References**

1. Serp, J.; Allibert, M.; Benes, O.; Delpech, S.; Feynberg, O.; Ghetta, V.; Heuer, D.; Holcomb, D.; Ignatiev, V.; Kloosterman, J. L.; Merle-Lucotte, L. L. E.; Uhlir, J.; Yoshioka, R.; Zhimin, D., The molten salt reactor (MSR) in generation IV: Overview and perspectives. *Prog. Nucl. Energy* **2014**, *77*, 308-319.
2. Mehos, M.; Turchi, C.; Vidal, J.; Wagner, M.; Ma, Z.; Ho, C.; Kolb, W.; Andraka, C.; Kruizenga, A. *Concentrating Solar Power Gen3 Demonstration Roadmap*; National Renewable Energy Laboratory: 2017.
3. Liu, M.; Tay, N. H. S.; Bell, S.; Belushko, M.; Jacob, R.; Will, G.; Saman, W.; Bruno, F., Review on concentration solar power plants and new developments in high temperature thermal energy storage technologies. *Renewable Sustainable Energy Rev.* **2016**, *53*, 1411-1432.
4. Kenisarin, M. M., High-Temperature phase change materials for thermal energy storage. *Renewable Sustainable Energy Rev.* **2010**, *14*, 955-970.
5. Sarbu, I.; Sebarchievici, C., A Comprehensive Review of Thermal Energy Storage. *Sustainability* **2018**, *10*, 191-222.

6. Yin, H.; Mao, X.; Tang, D.; Xiao, W.; Xing, L.; Zhu, H.; Wang, D.; Sadoway, D. R., Capture and electrochemical conversion of CO<sub>2</sub> to value-added carbon and oxygen by molten salt electrolysis. *Energy Environ. Sci.* **2013**, *6*, 1538-1545.
7. Angel G. Fernandez, J. G.-V., Eduard Oro, Alan Kruizenga, Aran Sole, Luisa F. Cabeza, Mainstreaming commercial CSP systems: A technology review. *J. Renewable Energy* **2019**, *140*, 152-176.
8. Gonzalez-Roubaud, E.; Perez-Osorio, D.; Prieto, C., Review of commercial thermal energy storage in concentrated solar power plants: Steam vs. molten salts. *Renewable Sustainable Energy Rev.* **2017**, *80*, 133-148.
9. Wang, K.; He, Y.-l., Thermodynamic analysis and optimization of a molten salt solar power tower integrated with a recompression supercritical CO<sub>2</sub> Brayton cycle based on integrated modeling. *Energy Convers. Manage.* **2017**, *135*, 336-350.
10. McMurray, J. W.; Johnson, K.; Agca, C.; Betzler, B. R.; Kropaczek, D. J.; Besmann, T. M.; Andersson, D.; Ezell, N. *Roadmap for thermal property measurements of Molten Salt Reactor systems*; ORNL/SPR-2020/1865; Oak Ridge National Lab.(ORNL), Oak Ridge, TN (United States): 2021.
11. Bonk, A.; Sau, S.; Uranga, N.; Hernaiz, M.; Bauer, T., Advanced heat transfer fluids for molten salt line-focusing CSP. *Prog. Energy Combust. Sci.* **2018**, *67*, 69-87.
12. Nunes, V. M. B.; Queiros, C. S.; Lourenco, M. J. V.; Santos, F. J. V.; Nieto de Castro, C. A., Molten salts as engineering fluids - A review Part I. Molten alkali nitrates. *Appl. Energy* **2016**, *183*, 603-611.
13. Nunes, V. M. B.; Lourenco, M. J. V.; Santos, F. J. V.; Nieto de Castro, C. A., Importance of Accurate Data on Viscosity and Thermal Conductivity in Molten Salts Applications. *J. Chem. Eng. Data* **2003**, *48*, 446-450.
14. Williams, D. F.; Toth, L. M.; Clarno, K. T. *Assessment of Candidate Molten Salt Coolants for the Advanced High-Temperature Reactor (AHTR)*; ORNL/TM-2006/12; Oak Ridge National Laboratory: 2006.
15. Serrano-Lopez, R.; Fradera, J.; Cuesta-Lopez, S., Molten salts database for energy applications. *Chem. Eng. Process.* **2013**, *73*, 87-102.
16. Magnusson, J.; Memmott, M.; Munro, T., Review of thermophysical property methods applied to fueled and un-fueled salts. *Ann. Nucl. Energy* **2020**, *146*.
17. Bauer, T.; Pfleger, N.; Breidenbach, N.; Eck, M.; Laing, D.; Kaesche, S., Material Aspects of Solar Salt for sensible heat storage. *Appl. Energy* **2013**, *111*, 1114-1119.
18. Sharma, S.; Ivanov, A. S.; Margulis, C., A Brief Guide to the Structure of High-Temperature Molten Salts and Key Aspects Making Them Different from Their Low-Temperature Relatives, the Ionic Liquids. *J. Phys. Chem. B* **2021**, *125*, 6359-6372.
19. Grosu, Y.; Gonzalez-Fernandez, L.; Nithyanantham, U.; Faik, A., Wettability Control for Correct Thermophysical Properties Determination of Molten Salts and Their Nanofluids. *Energies* **2019**, *12*, 3765-3777.
20. Agca, C.; McMurray, J. W., Empirical estimation of densities in NaCl-KCl-UCI<sub>3</sub> and NaCl-KCl-YCl<sub>3</sub> molten salts using Redlich-Kister expansion. *Chem. Eng. Sci.* **2022**, *247*.
21. McMurray, J. W. *Multi-Physics Simulations for Molten Salt Reactor Evaluation: Chemistry Modeling and Database Development*; ORNL/SPR-2018/864; Oak Ridge National Laboratory: 2018.
22. Benes, O.; Konings, R. J. M., Thermodynamic properties and phase diagrams of fluoride salts for nuclear applications. *J. Fluorine Chem.* **2009**, *130*, 22-29.
23. Romatoski, R. R.; Hu, L. W., Fluoride salt coolant properties for nuclear reactor applications: A review. *Ann. Nucl. Energy* **2017**, *109*, 635-647.
24. Ouyang, F.-Y.; Chang, C.-H.; You, B.-C.; Yeh, T.-K.; Kai, J.-J., Effect of Moisture on Corrosion of Ni-based alloys in molten alkali fluoride FLiNaK salt environments. *J. Nucl. Mater.* **2013**, *437*, 201-207.
25. Guo, S.; Zhang, J.; Wu, W.; Zhou, W., Corrosion in the molten fluoride and chloride salts and materials development for nuclear applications. *Prog. Mater. Sci.* **2018**, *97*, 448-487.

26. Cohen, S. I.; Jones, T. N. A Summary of Density Measurements on Molten Fluoride Mixtures and a Correlation for Predicting Densities of Fluoride Mixtures; Oak Ridge National Laboratory: 1954.

27. Grimes, W. R.; Cuneo, D. R.; Blankenship, F. F.; Keilholtz, G. W.; Poppendick, H. F.; Robinson, M. T., Chemical aspects of molten-fluoride-salt reactor fuels. In *Fluid Fueled Reactors*, Lane, J. A., Ed. Addison-Wesley: NY, 1958.

28. Powers, W. D.; Cohen, S. I.; Greene, N. D., Physical Properties of Molten Reactor Fuels and Coolants. *Nucl. Sci. Eng.* **1963**, 71, 200-211.

29. Vriesema, B. Aspects of Molten Fluorides as Heat Transfer Agents For Power Generation. Delft University of Technology, 1979.

30. Ambrosek, J.; Anderson, M.; Sridharan, K.; Allen, T., Current Status of Knowledge of the Fluoride Salt (FLiNaK) Heat Transfer *Nucl. Technol.* **2009**, 165.

31. Holcomb, D. E.; Cetiner, S. M. *An Overview of Liquid-Fluoride-Salt Heat Transport Systems*; ORNL/TM-2010/156; Oak Ridge National Laboratory: 2010.

32. Yoder, G., Examination of Liquid Fluoride Salt Heat Transfer. In *ICAPP 2014*, American nuclear Society: Charlotte, USA, 2014.

33. Mellors, G. W.; Senderoff, S. In *The Density and Surface Tension of Molten Fluorides*, Australian Conference on Electrochemistry, Sydney, Australia, J.A. Friend, F. G., Ed. Pergamon Press: Sydney, Australia, 1965.

34. Janz, G. J.; Tomkins, R. *Physical properties data compilations relevant to energy storage. IV. Molten salts: data on additional single and multi-component salt systems*; National Standard Reference Data System: 1981.

35. Chrenkova, M.; Daněk, V.; Silný, A.; Kremenetsky, V.; Polyakov, E., Density and viscosity of the (LiF-NaF-KF)<sub>eut</sub>-KBF<sub>4</sub>-B<sub>2</sub>O<sub>3</sub> melts. *J. Mol. Liq.* **2003**, 102, 213-226.

36. Cibulková, J.; Chrenkova, M.; Vasiljev, R.; Kremenetsky, V.; Boca, M., Density and viscosity of the (LiF+ NaF+ KF) eut (1)+ K<sub>2</sub>TaF<sub>7</sub> (2)+ Ta<sub>2</sub>O<sub>5</sub> (3) melts. *J. Chem. Eng. Data* **2006**, 51, 984-987.

37. An, X.-H.; Cheng, J.-H.; Su, T.; Zhang, P., Determination pf thermal physical properties of alkali fluoride/carbonate eutectic molten salt. *AIP Conf. Proc.* **2017**, 1850, 070001-1-7.

38. Jin-Hui, C.; Peng, Z.; Xue-Hui, A.; Kun, W.; Yong, Z.; Heng-Wei, Y.; Zhong, L., A device for measuring the density and liquidus temperature of molten fluorides for heat transfer and storage. *Chin. Phys. Lett.* **2013**, 30, 126501.

39. Rose, M. A.; Wu, E.; Williamson, M. A. *Thermophysical Property Measurements: Improved Density, Viscosity and Thermal Diffusivity Methods*; ANL/CFCT-20/38; 2020.

40. Barborik, P.; Vaskova, Z.; Boca, M.; Priscak, J., Physicochemical properties of the system(LiF + NaF + KF(eut.) + Na<sub>7</sub>Zr<sub>6</sub>F<sub>31</sub>): Phase equilibria, density and volume properties, viscosity and surface tension. *Zh. Khim. Termodin. Termokhim.* **2014**, 76, 145-151.

41. Cohen, S. I.; Jones, T. N. *Viscosity Measurements on Molten Fluoride Mixtures*; ORNL-2278; Oak Ridge National Laboratory: 1957.

42. Frandsen, B. A.; Nickerson, S. D.; Clark, A. D.; Solano, A.; Baral, R.; Williams, J.; Neuefeind, J.; Memmott, M., The structure of molten FLiNaK. *J. Nucl. Mater.* **2020**, 537, 152219.

43. Salanne, M.; Simon, C.; Turq, P.; Madden, P. A., Heat-transport properties of molten fluorides: Determination from first-principles. *J. Fluorine Chem.* **2009**, 130, 38-44.

44. Zhao, Y. *Molten Chloride Thermophysical Properties, Chemical Optimization, and Purification*; NREL/TP-5500-78047; National Renewable Energy Laboratory: 2020.

45. Shaffer, J. H. *Preparation and Handling of Salt Mixtures For the Molten Salt Reactor Experiment*; ORNL-4616; Oak Ridge National Laboratory: 1971.

46. Kelleher, B. C.; Dolan, K. P.; Brooks, P.; Anderson, M. H.; Sridharan, K., Batch-Scale Hydrofluorination of <sup>7</sup>Li<sub>2</sub>BeF<sub>4</sub> to Support Molten Salt Reactor Development. *J. Nucl. Eng. Radiat. Sci.* **2015**, 1.

47. Zong, G.; Zang, Z.-B.; Sun, J.-H.; Xiao, J.-C., Preparation of high-purity molten FLiNaK salt by the hydrofluorination process. *J. Fluorine Chem.* **2017**, *197*, 134-141.

48. Sulejmanovic, D.; Kurley, J. M.; Robb, K.; Raiman, S., Validating modern methods for impurity analysis in fluoride salts. *J. Nucl. Mater.* **2021**, *553*, 152972.

49. Chou, K.-C.; Hu, J.-H., A new experimental method for determining liquid density and surface tension. *Metall. Trans. B* **1991**, *22*, 27-31.

50. Kirby, R., Platinum—A thermal expansion reference material. *Int. J. Thermophys.* **1991**, *12*, 679-685.

51. Redlich, O.; Kister, A., Algebraic representation of thermodynamic properties and the classification of solutions. *Ind. Eng. Chem. Res.* **1948**, *40*, 345-348.

52. Kubíková, B.; Mlynáriková, J.; Wu, S.; Mikšíková, E.; Priščák, J.; Boča, M.; Korenko, M., Physicochemical Investigation of the Ternary (LiF+ MgF<sub>2</sub>) eut+ LaF<sub>3</sub> Molten System. *J. Chem. Eng. Data* **2020**, *65*, 4815-4826.

53. Mlynáriková, J.; Boča, M.; Mikšíková, E.; Netriová, Z., Volume properties of the molten systems MF-K 2 TaF 7 (MF= LiF, NaF and KF). *J. Therm. Anal. Calorim.* **2017**, *129*, 475-486.

54. McMurray, J. W.; Besmann, T. M. *Thermodynamic Modeling of Nuclear Fuel Materials*; Oak Ridge National Lab.(ORNL), Oak Ridge, TN (United States): 2018.

55. Kubíkova, B.; Boča, M.; Mlynáriková, J.; Gurišová, V.; Šimurda, M.; Netriová, Z.; Korenko, M., Physicochemical properties of the (LiF+ CaF<sub>2</sub>) eut+ LaF<sub>3</sub> system: phase equilibria, volume properties, electrical conductivity, and surface tension. *J. Chem. Eng. Data* **2016**, *61*, 1395-1402.

56. Guo, C.; Du, S.; Lu, H.; Zhao, L.; Tang, D., Density and Viscosity of NdF<sub>3</sub>-LiF-BaF<sub>2</sub> Molten Salt. *J. Chinese Rare Earth Soc.* **1989**, *7*, 7-11.

57. Levenberg, K., A method for the solution of certain non-linear problems in least squares. *Q. Appl. Math.* **1944**, *2*, 164-168.

58. Marquardt, D. W., An algorithm for least-squares estimation of nonlinear parameters. *J. Soc. Ind. Appl. Math.* **1963**, *11*, 431-441.

59. Taniuchi, K.; Kanai, T., Density of Binary Molten-Salts of Lithium-Fluoride Potassium Fluoride and Lithium Fluoride Calcium Fluoride Systems. *Denki Kagaku* **1977**, *45*, 401-404.

60. Porter, B.; Meaker, R. E., *Density and molar volumes of binary fluoride mixtures*. US Department of the Interior, Bureau of Mines: 1966; Vol. 6836.

61. Janz, G. J., Thermodynamic and transport properties for molten salts: correlation equations for critically evaluated density, surface tension, electrical conductance, and viscosity data. *J. Phys. Chem. Ref. Data* **1988**, *17*.

62. Danielik, V.; Gabčová, J., Phase diagram of the system NaF-KF-AlF 3. *J. Therm. Anal. Calorim.* **2004**, *76*, 763-773.